CHINESE OPTICS LETTERS

Vol. 22, No. 5 | May 2024

Polarization-entangled photon pairs with factorable spectra engineered by using an uneven four-stage nonlinear interferometer

Liang Cui (崔 亮)[1], Haoran Chen (陈浩然)[1], Jiamin Li (李嘉敏)[1,2], and Xiaoying Li (李小英)[1*]

[1] College of Precision Instrument and Opto-Electronics Engineering, Key Laboratory of Opto-Electronics Information Technology, Ministry of Education, Tianjin University, Tianjin 300072, China

[2] School of Physics, Taiyuan University of Technology, Taiyuan 030000, China

*Corresponding author: xiaoyingli@tju.edu.cn

Received October 18, 2023 | Accepted January 15, 2024 | Posted Online May 14, 2024

We report the generation of polarization-entangled photon pairs in the 1550 nm band by pumping an uneven nonlinear interferometer loop with two orthogonally polarized counterpropagating pump pulses. The uneven nonlinear interferometer, providing a more ideal interference pattern due to the elimination of secondary maxima, consists of four pieces of dispersion-shifted fibers sandwiched with three pieces of standard single-mode fibers, and the lengths of the nonlinear fibers follow the binomial distribution. The mode number of the photon pairs deduced from the measured joint spectrum is ~1.03. The collection efficiency of the photon pairs is found to be ~94% (after background noise correction). The directly measured visibility of two-photon interference of the polarization-entangled photon pairs is ~92%, while no interference is observed in the direct detection of either the signal or idler photons.

Keywords: polarization-entangled photon pairs; nonlinear interferometer; quantum state engineering; optical fiber.
DOI: 10.3788/COL202422.052701

1. Introduction

Quantum-entangled photon pair sources are essential resources for quantum information processing (QIP)[1]. Among various kinds of entangled degrees of freedom, such as polarization, orbital angular momentum, frequency, and temporal mode[2–4], the techniques for polarization control and manipulation are the most mature. Since the polarization entanglement was successfully generated via optical parametric processes in nonlinear media[2], it has been widely used in implementing various QIP tasks. On the other hand, for many applications involving two-photon interference between independent sources, such as quantum teleportation[5], entanglement swapping[6], and multiphoton entanglement generation[7], entangled photon pairs in pure single mode and with high collection efficiency are desirable. Single-mode operation requires complete elimination of the spectral and spatial correlations between the entangled signal and idler photons. By using $\chi^{(2)}$ or $\chi^{(3)}$ nonlinear waveguides supporting a single spatial mode, the spatial correlation can be straightforwardly eliminated[2,8]. However, it is nontrivial to get rid of the spectral correlation without sacrificing collection efficiency[9,10]. Exquisite efforts have been made in solving the problem[11–18]. When a single-piece nonlinear medium is used, frequency de-correlated, namely, spectrally factorable, photon pairs can be achieved only at some specific wavelengths with sophisticated dispersion design because the spectral tailoring and phase matching are mixed in parametric processes[13–16].

To engineer the mode structure of the quantum states, it has been proposed that precise state engineering for near ideal single mode operation and near unity efficiency can be achieved by using SU(1,1) nonlinear interferometers (NLIs)[19–21]. Since the interferometric method separates the spectral control from the phase matching of the nonlinear process, photon pairs simultaneously possess the features of high purity and high collection efficiency, and high flexibility in wavelength and bandwidth selection can be generated. In particular, we have experimentally demonstrated the generation of spectrally factorable photon pairs using a fiber-based NLI, formed by a sequential array of identical nonlinear fibers with a gap in between made of a linear dispersive medium. The heralding efficiency and the visibility of two-photon interference between two independent sources of heralded single photons could be simultaneously greater than 90%[22]. However, the achievable factorability is limited due to the secondary maxima between the principal maxima of the interference term, $\sin(N\theta)/\sin\theta$, where θ is the phase shift induced by the dispersive media in the NLI[19].

In this paper, we show that the secondary maxima in the interference term can be eliminated by using an uneven

four-stage NLI. The length ratio of the four nonlinear fibers in the NLI is 1:3:3:1, which follows the binomial distribution[20,23]. In this case, the parametric gain is varied in each stage and results in a more ideal interference pattern. By simultaneously pumping such an uneven NLI loop with two orthogonally polarized counterpropagating pulse trains, we generate polarization-entangled photon pairs with improved mode purity and collection efficiency.

2. Method

Our experimental setup is shown in Fig. 1. The uneven four-stage NLI is formed by four pieces of dispersion-shifted fibers (DSFs) with three pieces of standard single-mode fibers (SMFs) in between. The DSFs with zero dispersion wavelength and dispersion slope of 1549 nm and 0.0075 ps/(km · nm^2), respectively, function as the nonlinear media of four-wave mixing (FWM). The lengths of DSF1, DSF2, DSF3, and DSF4 are 50, 150, 150, and 50 m, respectively. In the pump-degenerate FWM process, two photons with frequency ω_p from the pump field are scattered into a pair of correlated signal and idler photons with frequency ω_s and ω_i, respectively, and energy conservation $2\omega_p = \omega_s + \omega_i$ is satisfied. Because of the isotropic nature of the $\chi^{(3)}$ nonlinearity in silica fibers, the photon pairs are predominantly co-polarized with the pump. The SMFs function as linear dispersive media and have the same length of 20 m. We submerge the NLI into liquid nitrogen to suppress the photons from spontaneous Raman scattering (RS)[24]. The transmission efficiency of the NLI is ~41%, and the interstage efficiency is ~74%. The loss is mostly due to the splicing loss between the DSFs and SMFs, which is ~0.6 dB per splicing point.

The pulsed pump originates from a mode-locked fiber laser and is filtered by a Gaussian-shaped bandpass filter (not shown in the setup). The repetition rate of the pulse train is 50 MHz. The central wavelength and bandwidth of the nearly transform-limited pump pulses are 1549.3 and 1.4 nm, respectively.

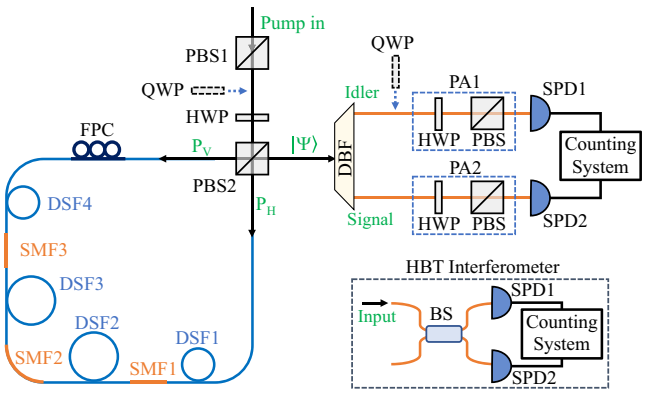

Fig. 1. Experimental setup for generating polarization-entangled state by using a four-stage uneven NLI. DSF, dispersion shifted fiber; SMF, single-mode fiber; PBS, polarization beam splitter; QWP, quarter-wave plate; HWP, half-wave plate; FPC, fiber polarization controller; DBF, dual-band filter; PA, polarization analyzer; SPD, single-photon detector.

The pump is passed through a polarization beam splitter (PBS), PBS1, to ensure its horizontal polarization. By adjusting the half-wave plate (HWP) placed in front of PBS2, the pump is equally decomposed into horizontally and vertically polarized components P_H and P_V, respectively. The component P_H propagating clockwise in the NLI produces correlated photon pairs $|H\rangle_s|H\rangle_i$, whereas P_V propagating counterclockwise produces $|V\rangle_s|V\rangle_i$. A fiber polarization controller (FPC) is used to compensate for the birefringence introduced by the bending and coiling of the NLI loop. The correlated wave packets $|H\rangle_s|H\rangle_i$ and $|V\rangle_s|V\rangle_i$ are coherently combined at PBS2; then, the polarization-entangled state $|\Psi\rangle = \frac{1}{\sqrt{2}}(|H\rangle_s|H\rangle_i + e^{i\phi}|V\rangle_s|V\rangle_i)$ is created, where ϕ is the phase difference between the two wave packets[25,26]. For the above described setup, we have $\phi = 2\phi_p$, where ϕ_p is the relative phase between P_H and P_V and equals zero. So, the obtained state is $|\Psi^+\rangle = \frac{1}{\sqrt{2}}(|H\rangle_s|H\rangle_i + |V\rangle_s|V\rangle_i)$.

To reliably detect the entangled signal and idler photons, a high pump-to-signal rejection ratio is required. In our NLI, about 0.03 photon pairs are produced within a typical 2.5-ps-duration pump pulse containing 10^7 photons. By passing the output of PBS2 through a dual-band filter (DBF), we can separate the photon pairs from the pump with an isolation greater than 100 dB. The DBF consists of a notch filter and a programmable optical filter (Finisar Waveshaper 4000), which has two tunable rectangle-shaped passbands. With the DBF, we can realize single-channel or joint spectral scan measurements. To characterize the polarization entanglement, we place two polarization analyzers (PA1 and PA2) in the signal and idler channels, respectively. Each PA consists of an HWP and a PBS. The photons are detected by using two superconducting nanowire single-photon detectors (SPDs) with quantum efficiency of 85%. The total detection efficiencies of the signal and idler photons, η_s and η_i, are both ~12% (including transmission efficiency in the NLI, efficiencies of the filters and analyzers, and quantum efficiency of the SPDs).

When analyzing state $|\Psi\rangle = \frac{1}{\sqrt{2}}(|H\rangle_s|H\rangle_i + e^{i\phi}|V\rangle_s|V\rangle_i)$, the single-channel photon counts in the signal (idler) channel can be expressed as $\frac{1}{2}\eta_{s(i)}\alpha$, and the true coincidence counts of the entangled photon pairs can be expressed as[26]

$$C_t = \frac{1}{2}\eta_c\eta_s\eta_i\alpha(\cos^2\theta_1\cos^2\theta_2 + \sin^2\theta_1\sin^2\theta_2 + 2\cos\phi\sin\theta_1\sin\theta_2\cos\theta_1\cos\theta_2), \quad (1)$$

where α is the rate of photon pairs produced from NLI, η_c is the collection efficiency of the entangled photon pairs, and θ_1 and θ_2 are the angles of PA1 and PA2, respectively.

3. Results

We first characterize the spectral profile of the entangled photon pairs. Under the approximation of perfect phase matching of FWM, the joint spectral function of the photon pairs from an uneven N-stage NLI can be expressed as[20,23]

$$F_{\mathrm{NLI}}(\omega_s,\omega_i) \propto \exp\left[-\frac{(\omega_s+\omega_i-2\omega_{p0})^2}{4\sigma_p^2}\right]\times\cos^{2(N-1)}\theta, \quad (2)$$

where ω_{p0} and σ_p are the central wavelength and bandwidth of the pump, respectively. The phase shift is introduced by the SMFs $\theta \approx \lambda_{p0}^2 D_{\mathrm{SMF}} L_{\mathrm{SMF}}(\omega_s-\omega_i)^2/(16\pi c)$, where $D_{\mathrm{SMF}} = 17\,\mathrm{ps}/(\mathrm{nm}\cdot\mathrm{km})$ is the dispersion of SMF at the pump wavelength λ_{p0}, and L_{SMF} is the length of each SMF. Just as the multi-slit interference in classical optics, the interference term of an even NLI can be expressed as $\sin(N\theta)/\sin\theta$, which means there are secondary maxima occurring between the primary maxima. In contrast, the interference term $\cos^{2(N-1)}\theta$ in Eq. (2) has no secondary maximum. The calculated joint spectral intensity (JSI) $|F_{\mathrm{NLI}}(\omega_s,\omega_i)|^2$ of the photon pairs from our NLI is shown in Fig. 2(a). One sees that there is no secondary island between two adjacent principal islands, which is different from the pattern in Ref. [22], and the island labeled $m=1$ is round-shaped. Once we carve out the $m=1$ island by using rectangle-shaped bandpass filters with proper bandwidths [see the dashed lines in Fig. 2(a)], photon pairs with factorable spectra can be obtained. After performing a mode decomposition on the joint spectral function, we find the calculated mode number K of the carved-out photon pairs is ~1.01, which is very close to the single-mode case.

We experimentally measure the JSI of the polarization-entangled photon pairs from the NLI loop. In the experiment, the average power P_{ave} of both pumps P_H and P_V is fixed at 60 μW, the bandwidth of the DBF is adjusted to 0.2 nm, and the angles of PA1 and PA2 are both set to 45°. We scan the central wavelength of the signal (idler) channel of the DBF from 1553.0 nm (1545.4 nm) to 1558.2 nm (1540.2 nm) with a step of 0.2 nm. For each wavelength setting, we record the twofold coincidence counts C_c and accidental coincidence counts C_a of the signal and idler photons, which are obtained by measuring the signal and idler photons from the same pump pulse and adjacent pump pulses, respectively. Then we can deduce the true coincidence counts $C_t = C_c - C_a$. The contour map of measured C_t is plotted in Fig. 2(b), which reflects the JSI of the entangled photon pairs. One sees that the measured JSI agrees well with the calculated result in Fig. 2(a), and the $m=1$ island centering at $\lambda_s = 1554.1$ nm and $\lambda_i = 1544.5$ nm has a round shape.

Next, we carve out the $m=1$ island for further characterization. The central wavelengths of the signal and idler channels of the DBF are adjusted to 1554.1 and 1544.5 nm, respectively, and the bandwidth of both channels is set to 2.2 nm. We first measure the collection efficiency of the photon pairs. In the measurement, we change the average power P_{ave} of the two pumps, and record the single counts $R_{s(i)}$ of individual signal (idler) field and the true coincidence counts C_t. The main and inset plots of Fig. 3(a), respectively, show the measured R_i and C_t versus P_{ave}. We fit the measured R_i with polynomial $s_1 P_{\mathrm{ave}} + s_2 P_{\mathrm{ave}}^2$, where s_1 and s_2 are fitting parameters. The linear and quadratic terms $s_1 P_{\mathrm{ave}}$ and $s_2 P_{\mathrm{ave}}^2$ represent the photons from spontaneous RS and FWM, respectively. The RS photons can be seen as noise, so we can subtract them from the signal channel counts. Using Eq. (1), we can deduce the collection efficiency of the entangled photon pairs via $\eta_c = \frac{C_t}{\eta_s s_2 P_{\mathrm{ave}}^2}$. After substituting the measured and fitted results, we find the collection efficiency η_c is ~94%.

We then measure the second-order intensity correlation function $g^{(2)}$ of the individual signal or idler field to examine the mode purity. $g^{(2)}$ is related to mode number K via $g^{(2)} = 1 + 1/K$. The inset of Fig. 3(b) shows the measured $g^{(2)}$ of the individual idler field, which is obtained by sending the output of PA1 into the HBT interferometer (see inset of Fig. 1). One sees that the measured $g^{(2)}$ increases with pump power P_{ave} because the proportions of photons originated from RS and FWM vary. We extract the correlation function of photons from FWM by utilizing the method in Ref. [27]. First, we replot the measured $g^{(2)}$ as a function of the proportion of FWM photons in the idler field $\mathcal{R} = s_2 P_{\mathrm{ave}}^2/R_i$, as shown by the data points in the main plot in Fig. 3(b). Note that $\mathcal{R}=0$ and $\mathcal{R}=1$, respectively, correspond to the correlation functions of photons exclusively from RS and FWM, namely, $g^{(2)}_{\mathrm{RS}}$ and $g^{(2)}_{\mathrm{FWM}}$. We obtain $g^{(2)}_{\mathrm{RS}} = 1.52$ by only sending P_H into the NLI, connecting the output port of the FPC directly to the DBF, and selecting the photons cross-polarized with pump by adjusting PA1. In this condition, photons from FWM are blocked, and all the photons sent into the HBT interferometer are from RS[28]. We then fit the data points in Fig. 3(b) with function[27] $g^{(2)} = 1 + \mathcal{R}^2(g^{(2)}_{\mathrm{FWM}} - 1) + (1-\mathcal{R})(1-\mathcal{R}+2\mathcal{V}\mathcal{R})(g^{(2)}_{\mathrm{RS}} - 1)$, where $\mathcal{V}$

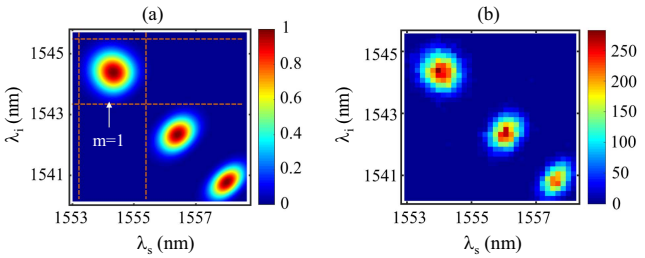

Fig. 2. (a) Theoretically calculated and (b) experimentally measured joint spectral intensity of the entangled photon pairs.

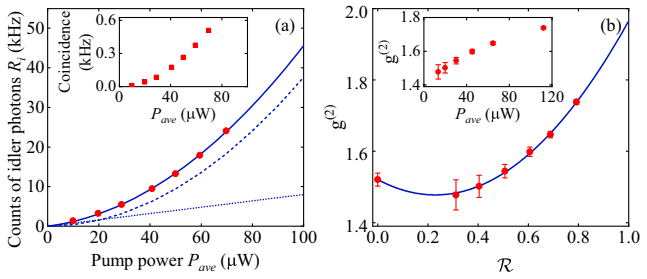

Fig. 3. (a) Measured count rate of idler photons R_i versus average pump power P_{ave}. Inset: measured true coincidence C_t versus P_{ave}. The solid line represents the fitting polynomial $R_i = s_1 P_{\mathrm{ave}} + s_2 P_{\mathrm{ave}}^2$, where s_1 and s_2 are the fitting parameters. The dotted line and dashed line are the linear and quadratic terms, respectively. (b) Measured intensity correlation function of the idler field $g^{(2)}$ versus proportion of photons from FWM, $\mathcal{R} = s_2 P_{\mathrm{ave}}^2/R_i$. Inset: measured $g^{(2)}$ versus pump power P_{ave}.

describes the mode overlap between the FWM and RS photons. From the fitting result shown by the solid curve, we deduce the intensity correlation of the FWM photons $g^{(2)}_{\mathrm{FWM}} = 1.97$, which corresponds to a mode number of ~1.03. The measured mode purity is in accordance with the simulated result using the calculated joint spectral function. We think that the deviation is mainly due to the chirp existing in pump pulses.

We measure the two-photon interference (TPI) of the entangled photon pairs. In the measurement, the average power P_{ave} of both pumps is 60 μW. For state $|\Psi^+\rangle = \frac{1}{\sqrt{2}}(|H\rangle_s|H\rangle_i + |V\rangle_s|V\rangle_i)$, we fix the angle of PA1 θ_1 at 45° relative to the horizontal polarization defined by the PBS connecting the loop, while the angle of PA2 θ_2 is varied. For each setting of $\theta_1 - \theta_2$, we record the single-channel counts and coincidence counts of the two SPDs. The results are shown in Fig. 4. One sees that interference pattern exists in the coincidence counts, whereas no interference is observed in the single counts. By fitting the coincidence with the cosine function in Eq. (1), we find that the TPI visibility is 92%, without subtracting the noise and dark counts of the SPDs. Note that our source can produce all four polarization-entangled Bell states. By inserting a quarter-wave plate (QWP) (see Fig. 1) with its axis parallel to PBS1, we have $\phi_p = \pi/2$. In this case, the state at the output of PBS2 becomes $|\Psi^-\rangle = \frac{1}{\sqrt{2}}(|H\rangle_s|H\rangle_i + |V\rangle_s|V\rangle_i)$. The other two Bell states $|\Phi^\pm\rangle = \frac{1}{\sqrt{2}}(|H\rangle_s|V\rangle_i \pm |V\rangle_s|H\rangle_i)$ can also be created when $\phi_p = 0$ or $\pi/2$ and a properly oriented HWP is placed in front of PA1 in the idler channel.

Moreover, we experimentally characterize the influence of interstage loss on the performance of the NLI scheme. We prepare two uneven NLIs for the characterization. One is a three-stage NLI in which the lengths of DSFs are 50, 100, and 50 m, respectively; the other is a four-stage NLI in which the lengths of DSFs are 50, 150, 150, and 50 m. The lengths of all SMFs in the two NLIs are 20 m. We apply an adjustable attenuator on each SMF so that the interstage efficiency can be controlled. In the experiment, we employ the DBF as a tunable filter and use the same method as that in the JSI measurement. First, we measure the spectra of idler photons from the two NLIs by recording the single-channel photon counting rates as a function of idler wavelength, and we repeat the measurement at different pump powers. Then, by using the fitting method shown in Fig. 3(a), we extract the spectra of idler photons solely from spontaneous FWM.

Figure 5 shows the obtained spectra from the two NLIs when the interstage efficiency η_{inter} is 40% and 78%, respectively. The measurement is conducted at room temperature; compared with the case of submerging the NLI in liquid nitrogen, the zero-dispersion wavelength of the DSFs shifts towards the longer wavelength. To achieve the best phase-matching condition, we increase the pump wavelength by 5.6 nm to 1554.9 nm. Therefore, the wavelengths of the maxima and minima in the measured spectra accordingly shift by about 5.6 nm compared with the results in Fig. 2. By fitting the measured data and examining the $m = 1$ island, we can get the visibility of nonlinear interference fringes. From the results of both NLIs, one can see that the visibility drops sharply as η_{inter} changes from 78% to 40%, accompanied by the huge decrease of the photon counting rates. Comparing the three- and four-stage cases, one sees that the visibility in the four-stage case is significantly higher, which is because the islands become more isolated[20]. Moreover, the influence of η_{inter} on the fringe visibility is less significant for NLI with a larger stage number. However, on the other hand, the interstage loss accumulates as the stage number increases, which results in a decreased efficiency of the source. This can be revealed by that the total length of DSFs in the four-stage NLI is 2 times that in the three-stage NLI, but photon counting rates of both cases are at the same level.

Our investigation shows that to further improve the mode purity and collection efficiency of the entangled photon pairs,

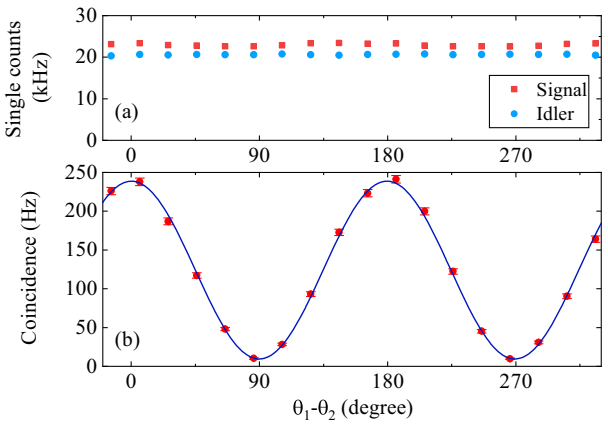

Fig. 4. Measured (a) single-channel counts and (b) coincidence counts versus the relative angle θ_1–θ_2 of the two polarization analyzers. The solid curve in (b) is the fitting cosine function, which corresponds to a TPI visibility of 92%.

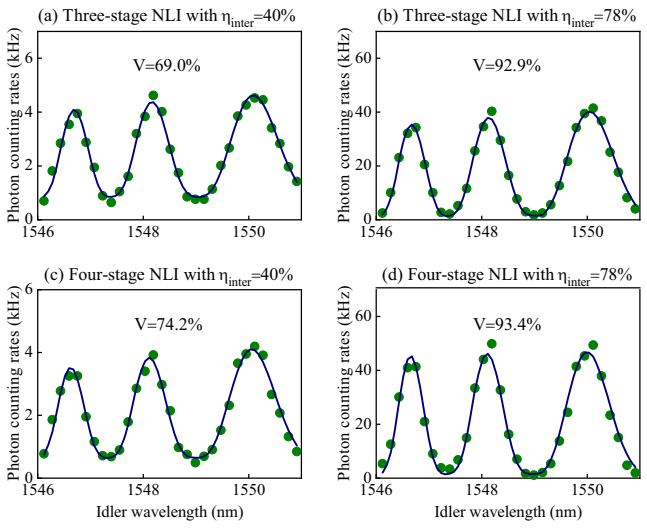

Fig. 5. Spectra of idler photons generated from spontaneous FWM in uneven NLIs. (a) and (b) are the results of three-stage NLI with interstage efficiencies of 40% and 78%, respectively. (c) and (d) are the results of four-stage NLI. The points are measured data, while the curves are fitting results. The visibility of interference fringe V is obtained from the leftmost island in each plot.

the interstage loss should be as low as possible. In the current setup, the splicing loss between DSF and SMF is relatively high. However, new fusion techniques such as tapering and flattening have been developed, and the splicing loss between DSF and SMF can be reduced to about 0.13 dB per slicing point or less[29]. Our scheme can be further improved by utilizing these techniques.

4. Conclusion

In conclusion, we have demonstrated a source of polarization-entangled photon pairs by employing an uneven four-stage NLI loop, which consists of four DSFs with three standard SMFs in between. The spectral factorability of the entangled photon pairs is realized by exploiting the active filtering effect of the NLI. Because the lengths of the DSFs follow the binomial distribution, the active filtering of our NLI is more ideal than that of an even NLI with the same stage number but with each DSF having identical length[22]. Experimental results indicate that the mode number of photon pairs is ∼1.03, while the collection efficiency of photon pairs is ∼94% (after correcting influences of the RS photons and detection efficiency). The directly measured two-photon interference visibility of the entangled state is ∼92%. Such a source can be further developed into an all-fiber device if the fiber length in the NLI is properly designed so that the wavelength and bandwidth of the photon pairs match the standard components of a fiber communication system. Compared with previous fiber sources of polarization-entangled photon pairs at 1550 nm band[25,26,30,31], our source simultaneously has the advantage of mode purity and high collection efficiency. We also find that the interstage loss in the NLI is a crucial factor for the performance of the scheme. Reducing the interstage loss can dramatically increase the visibility of the nonlinear interference, which can lead to higher modal purity. Moreover, our uneven NLI scheme can also be transplanted to other platforms, such as integrated nonlinear waveguides, to realize a miniaturized source of entangled photon pairs with tailored joint spectra.

Acknowledgements

This work was supported by the National Natural Science Foundation of China (Nos. 12074283, 91836302, 11874279, and 62305240).

References

1. S. Slussarenko and G. J. Pryde, "Photonic quantum information processing: a concise review," Appl. Phys. Rev. **6**, 041303 (2019).
2. P. G. Kwiat, K. Mattle, H. Weinfurter, *et al.*, "New high-intensity source of polarization-entangled photon pairs," Phys. Rev. Lett. **75**, 4337 (1995).
3. M. Krenn, M. Malik, M. Erhard, *et al.*, "Orbital angular momentum of photons and the entanglement of Laguerre-Gaussian modes," Philos. Trans. R. Soc. A **375**, 20150442 (2017).
4. B. Brecht, D. V. Reddy, C. Silberhorn, *et al.*, "Photon temporal modes: a complete framework for quantum information science," Phys. Rev. X **5**, 041017 (2015).
5. D. Bouwmeester, J.-W. Pan, K. Mattle, *et al.*, "Experimental quantum teleportation," Nature **390**, 575 (1997).
6. J.-W. Pan, D. Bouwmeester, H. Weinfurter, *et al.*, "Experimental entanglement swapping: entangling photons that never interacted," Phys. Rev. Lett. **80**, 3891 (1998).
7. X.-L. Wang, L.-K. Chen, W. Li, *et al.*, "Experimental ten-photon entanglement," Phys. Rev. Lett. **117**, 210502 (2016).
8. X. Y. Li, P. L. Voss, J. E. Sharping, *et al.*, "Optical-fiber source of polarization-entangled photons in the 1550 nm telecom band," Phys. Rev. Lett. **94**, 053601 (2005).
9. W. P. Grice and I. A. Walmsley, "Spectral information and distinguishability in type-ii down-conversion with a broadband pump," Phys. Rev. A **56**, 1627 (1997).
10. Z. Y. Ou, "Parametric down-conversion with coherent pulse pumping and quantum interference between independent fields," J. Eur. Opt. Soc. Part B **9**, 599 (1997).
11. K. Garay-Palmett, H. J. McGuinness, O. Cohen, *et al.*, "Photon pair-state preparation with tailored spectral properties by spontaneous four-wave mixing in photonic-crystal fiber," Opt. Express **15**, 14870 (2007).
12. A. B. U'Ren, C. Silberhorn, K. Banaszek, *et al.*, "Generation of pure-state single-photon wavepackets by conditional preparation based on spontaneous parametiric downconversion," Laser Phys. **15**, 146 (2005).
13. P. J. Mosley, J. S. Lundeen, B. J. Smith, *et al.*, "Heralded generation of ultrafast single photons in pure quantum states," Phys. Rev. Lett. **100**, 133601 (2008).
14. P. G. Evans, R. S. Bennink, W. P. Grice, *et al.*, "Bright source of spectrally uncorrelated polarization-entangled photons with nearly single-mode emission," Phys. Rev. Lett. **105**, 253601 (2010).
15. L. Cui, X. Li, and N. Zhao, "Minimizing the frequency correlation of photon pairs in photonic crystal fibers," New J. Phys. **14**, 123001 (2012).
16. A. M. Branczyk, A. Fedrizzi, T. M. Stace, *et al.*, "Engineered optical nonlinearity for quantum light sources," Opt. Express **19**, 55 (2011).
17. R.-B. Jin, R. Shimizu, K. Wakui, *et al.*, "Pulsed Sagnac polarization-entangled photon source with a PPKTP crystal at telecom wavelength," Opt. Express **22**, 11498 (2014).
18. R.-B. Jin, R. Shimizu, M. Fujiwara, *et al.*, "Simple method of generating and distributing frequency-entangled qudits," Quantum Sci. Technol. **1**, 015004 (2016).
19. J. Su, L. Cui, J. Li, *et al.*, "Versatile and precise quantum state engineering by using nonlinear interferometers," Opt. Express **27**, 20479 (2019).
20. L. Cui, J. Su, J. Li, *et al.*, "Quantum state engineering by nonlinear quantum interference," Phys. Rev. A **102**, 033718 (2020).
21. L. Cui, J. Wang, J. Li, *et al.*, "Programmable photon pair source," APL Photonics **7**, 016101 (2022).
22. J. Li, J. Su, L. Cui, *et al.*, "Generation of pure-state single photons with high heralding efficiency by using a three-stage nonlinear interferometer," Appl. Phys. Lett. **116**, 204002 (2020).
23. M. Ma, L. Cui, and X. Li, "Engineering the spectral profile of photon pairs by using multi-stage nonlinear interferometers," Chin. Opt. Lett. **19**, 052702 (2021).
24. X. Y. Li, J. Chen, P. Voss, *et al.*, "All-fiber photon-pair source for quantum communications: improved generation of correlated photons," Opt. Express **12**, 3737 (2004).
25. H. Takesue and K. Inoue, "Generation of polarization-entangled photon pairs and violation of Bell's inequality using spontaneous four-wave mixing in a fiber loop," Phys. Rev. A **70**, 031802 (2004).
26. X. Li, C. Liang, K. Fook Lee, *et al.*, "Integrable optical-fiber source of polarization-entangled photon pairs in the telecom band," Phys. Rev. A **73**, 052301 (2006).
27. J. Su, J. Li, L. Cui, *et al.*, "Interference between two independent multi-temporal-mode thermal fields," Phys. Rev. A **99**, 013838 (2019).
28. N. Liu, J. Su, Y. Liu, *et al.*, "Temporal mode properties of raman scattering in optical fibers," Opt. Express **29**, 13408 (2021).
29. A. Martinez-Rios, I. Torres-Gomez, D. Monzon-Hernandez, *et al.*, "Reduction of splice loss between dissimilar fibers by tapering and fattening," Rev. Mex. Fis. **56**, 80 (2010).
30. C. Chen, A. Riazi, E. Y. Zhu, *et al.*, "Turn-key diode-pumped all-fiber broadband polarization-entangled photon source," OSA Contin. **1**, 981 (2018).
31. F. Zhu, W. Zhang, and Y. Huang, "Fiber-based frequency-degenerate polarization entangled photon pair sources for information encoding," Opt. Express **24**, 25619 (2016).